Research Article

Advances in Mechanical Engineering

Advances in Mechanical Engineering
2016, Vol. 8(8) 1–9

DOI: 10.1177/1687814016659181
aime.sagepub.com
SAGE

Vertical random vibration analysis of adjacent building induced by highway traffic load

Wentao Xu[1], Yongjie Chen[1], Pan Xiang[2], Jianbo Zhang[1] and David Kennedy[3]

Abstract

Vehicle–pavement coupling systems may produce strong vertical random vibration due to the road surface unevenness and then further induce random vibration of adjacent buildings. It is usually difficult to numerical analyze efficiently as the model precision and calculation scale of complicated random analysis. In this article, a longitudinal infinite Kirchhoff plate with Kelvin foundation is employed to model the pavement system, and by proving the symplectic orthogonal characteristic for the damped chain substructure, the infinitely long road surface is regarded as a periodic chain-type substructure, the model is accurate, and computation scale is reduced. Models of a half vehicle and an adjacent building are coupled to the plate to produce a unified finite element model. The plate element stiffness matrix is formulated in the coordinate moving with the load, a typical model of road substructure is built, and the two-dimensional moving element method of vertical coupling random vibration is formulated, and then the time-varying non-stationary random vibration may be transformed into time-invariant stationary system. Using the pseudo-excitation method, vertical dynamic responses of the unified model of vibration source, supporting structure, and vibrated structure are analyzed. The computation efficiency of this method is numerically justified and some vibration influence rules of vehicle to building are drawn.

Keywords

Environmental vibration, chain substructure, pseudo-excitation method, moving element method, adjacent building

Date received: 15 March 2016; accepted: 13 June 2016

Academic Editor: Crinela Pislaru

Introduction

Complex urban transportation may have harmful influences on the surrounding residents and buildings, principally the environmental random vibrations induced by vehicle–pavement–structure coupling. Effectively reducing the influence of vibration and improving residential conditions are the key issues for sustainable transportation development.[1,2] Vehicle–pavement coupling vibrations induced by road surface irregularity are essentially random. This kind of coupled random vibration can induce the secondary vibrations of adjacent buildings by impact load spreading through the pavement structure, foundation, and the surrounding strata. This research field involves three areas: the random vibration of vehicle–pavement coupling systems, wave propagation in strata, and the secondary

[1]School of Mechanics and Engineering Science, Zhengzhou University, Zhengzhou, People's Republic of China
[2]State Key Laboratory of Structural Analysis for Industrial Equipment, Faculty of Vehicle Engineering and Mechanics, Dalian University of Technology, Dalian, People's Republic of China
[3]Cardiff School of Engineering, Cardiff University, Cardiff, UK

Corresponding author:
Wentao Xu, School of Mechanics and Engineering Science, Zhengzhou University, Zhengzhou 450001, People's Republic of China.
Email: xuwt@zzu.edu.cn

vibration of adjacent buildings, all of which are random and time-varying.

While many recent theoretical and numerical contributions have been made in the field, they mainly focus on the computing capability and efficiency of analysis methods. Hayakawa et al.[3] investigated the vibration characteristics of different parts of the vehicle, rail, bridges, and ground by establishing a numerical dynamic interaction analysis model of high-speed train-via-duct-foundation soil and using field tests of environmental vibration caused by the Shinkansen high-speed trains. Xu et al.[4] studied the effects of track irregularities on environmental vibration caused by underground railway and built a train–track–tunnel soil interaction model; the vibration acceleration and frequency distribution of ground surface were obtained. Alves et al.[5] presented a 2.5D finite element method (FEM)–boundary element method (BEM) model and a global description of a test site on a stretch of the Portuguese railway network. Xia and colleagues[6,7] researched environmental vibration caused by traffic systems, established a systematic analysis model of vehicle–structure–environment–building, and derived some rules for the propagation of the vibration in ground, underground, and elevated rail transit, including different terrains, speeds, and loads. By means of a vehicle–track–soil coupled vibration model based on vehicle–track dynamic theory, Zhai and colleagues[8,9] used the FEM to obtain the characteristics of soil deformation and vibration and an attenuation law at subcritical and near-critical speed. Yang and Hung[10] successfully proposed a 2.5D finite/infinite element procedure for dealing with the ground vibrations induced by moving loads, greatly reducing the numerical computation, and solved three-dimensional dynamic problems under train loads. Connolly et al.[11] evaluated the effect of vibrations on passenger comfort, followed by its effect on track performance; the ground-borne vibration was discussed along with its effect on the structural response of the building near railway lines. Tao and Wang[12] analyzed the environmental vibration caused by the railway and provided an effective method for the calculation of train random vibration load by combining the pseudo-excitation method (PEM) with the analytical model of vertical vibration of vehicle–pavement–foundation coupling.

It is concluded from these pioneering works in the field that the difficulties mainly focus on three aspects. The first difficulty is establishing a reasonable analytical model. The complete vibration system includes three basic subsystems, and each coupling relationship between the subsystems has its own characteristics. Vibration responses transferred with energy waves can lead to arbitrary energy dissipation if the subsystem models are analyzed separately. Second, the conventional methods for integrated system analysis are complicated and costly, which is particularly unacceptable when considering pavements of unlimited length and complex boundary conditions. Finally, it is difficult to accurately define the random characteristics of every subsystem.

To overcome these difficulties, in this article, an integrated model is recommended to analyze the environmental vibration caused by a vehicle–pavement coupling system, and a corresponding numerical analysis method is also developed based on the two-dimensional (2D) moving element method (MEM) and periodic chain substructure theory. Numerical examples justify the correctness and high efficiency of this new method, which is then used in the vertical random vibration analysis of an adjacent building.

Symplectic analysis of pavement periodic chain substructure

The integrated mechanical model for environmental vibration caused by the highway traffic load coupling system is shown in Figure 1.

An infinitely long Kirchhoff plate with a Kelvin foundation is employed to model the pavement and foundation structures. The vehicle is regarded as a half rigid model, and the wheels are assumed to remain in contact with the pavement at all times. Thus, the random vibration system can be coupled with the supporting pavement based on the displacement coordination condition. The adjacent building is modeled by the beams and columns, which couple with the supporting structure through elastic connections as shown in Figure 2.

Thus, the coupled dynamic model can describe the vehicle–pavement–building coupling random vibration system, which is a time-varying non-stationary multiexcitation random problem. Usually, the dynamic equation of the vehicle is deduced based on multi-body dynamics theory, D'Alembert's principle gives the differential equations of motion of the pavement, and the coupling dynamic equation is derived as equation (1) by displacement coordination condition between the wheel and pavement. Note that this section focuses on symplectic orthogonal characteristic for the damped chain substructure and gives the key equation only, because their derivation has been given elsewhere[13]

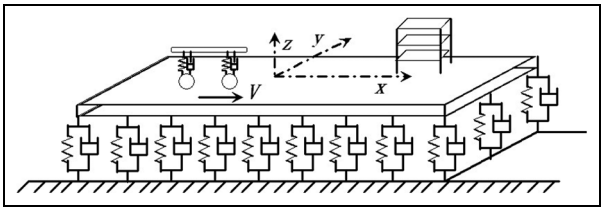

Figure 1. Integrated environmental vibration model.

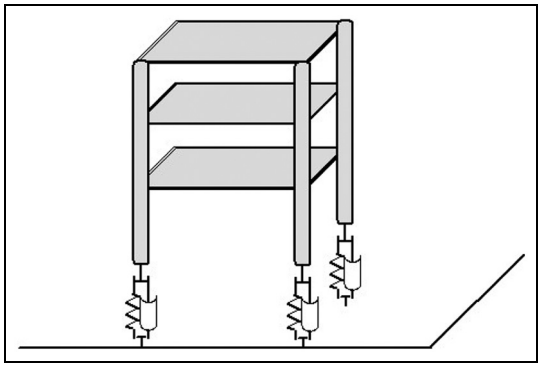

Figure 2. Coupled model of building structure and road foundation.

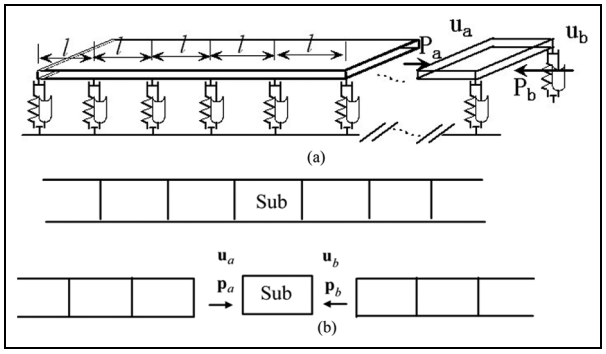

Figure 3. Periodic pavement substructure model: (a) stereoscopic sketch and (b) plan sketch.

$$\mathbf{M}\ddot{\mathbf{u}} + \mathbf{C}\dot{\mathbf{u}} + \mathbf{K}\mathbf{u} = \mathbf{F}(t) \tag{1}$$

in which the time-varying random excitation caused by pavement surface roughness is denoted as the vector $\mathbf{F}(t)$; the mass $\mathbf{M}$, damping $\mathbf{C}$, and stiffness $\mathbf{K}$ matrices include three parts: the mass $\mathbf{M}_d$, damping $\mathbf{C}_d$, and stiffness $\mathbf{K}_d$ matrices for the vehicle, respectively; $\mathbf{M}_u$, $\mathbf{C}_u$, and $\mathbf{K}_u$ for the pavement structures; the mass $\mathbf{M}_v$, damping $\mathbf{C}_v$, and stiffness $\mathbf{K}_v$ matrices for the adjacent building. In equation (1), these are coupled in random vibration with contact conditions between the vehicle and the pavement.

The pavement is usually considered as an infinitely long structure in engineering. In numerical simulation, the calculation of equation (1) is complicated and costly when considering an infinitely long pavement, whereas truncation error is obvious when considering just a part of the pavement structure. This section gives the well-established symplectic solution method for a periodic chain substructure and shows how it is applied to the infinite pavement structure. Figure 3 shows a periodic pavement substructure model, in which a harmonic wave with frequency ω is assumed to propagate.

The undamped equations of motion of the substructure have been proved in Lu et al.,[14] and the equations for hysteretic damping are

$$(e^{iv}\mathbf{K} - \omega^2\mathbf{M})\begin{Bmatrix}\mathbf{u}_i\\ \mathbf{u}_a\\ \mathbf{u}_b\end{Bmatrix} = \begin{bmatrix}\mathbf{K}^0_{ii} & \mathbf{K}^0_{ia} & \mathbf{K}^0_{ib}\\ (\mathbf{K}^0_{ia})^{\mathrm{T}} & \mathbf{K}^0_{aa} & \mathbf{K}^0_{ab}\\ (\mathbf{K}^0_{ib})^{\mathrm{T}} & (\mathbf{K}^0_{ab})^{\mathrm{T}} & \mathbf{K}^0_{bb}\end{bmatrix}\begin{Bmatrix}\mathbf{u}_i\\ \mathbf{u}_a\\ \mathbf{u}_b\end{Bmatrix} = \begin{Bmatrix}\mathbf{p}_{ie}\\ \mathbf{p}_{ae}\\ \mathbf{p}_{be}\end{Bmatrix} + \begin{Bmatrix}\mathbf{0}\\ \mathbf{p}_a\\ -\mathbf{p}_b\end{Bmatrix} \tag{2}$$

where the subscript a denotes the left ends of the substructure; similarly, b denotes the right and i the internal nodes. $\mathbf{u}_a$ and $\mathbf{u}_b$ are, respectively, the displacement vectors of the interface nodes at the left and right ends of the substructure and $\mathbf{u}_i$ is the displacement vector of the internal nodes; $\mathbf{K}^0_{xx}$ is the submatrix of the substructure matrix, the sum is 9, and subscript ii denotes the internal nodes of the submatrices, subscript ia is the submatrix between the nodes of left ends and internal, and the others are similar; $\mathbf{p}_{ae}$, $\mathbf{p}_{be}$, and $\mathbf{p}_{ie}$ are the corresponding external force vectors; $\mathbf{p}_a$ and $-\mathbf{p}_b$ are the interaction forces imposed by the adjacent substructures; T denotes the transpose of a matrix; $i = \sqrt{-1}$ and v is the hysteretic damping coefficient, so that e^{iv} is the hysteretic damping factor. For the coupled vehicle–pavement system, the mass $\mathbf{M}$ and stiffness $\mathbf{K}$ matrices are the same as those in equation (1). Eliminating the internal degree of freedom $\mathbf{u}_i$

$$\begin{bmatrix}\mathbf{K}_{aa} & \mathbf{K}_{ab}\\ \mathbf{K}^{\mathrm{T}}_{ab} & \mathbf{K}_{bb}\end{bmatrix}\begin{Bmatrix}\mathbf{u}_a\\ \mathbf{u}_b\end{Bmatrix} = \begin{Bmatrix}\mathbf{p}^*_a\\ \mathbf{p}^*_b\end{Bmatrix} + \begin{Bmatrix}\mathbf{p}_a\\ -\mathbf{p}_b\end{Bmatrix} \tag{3}$$

$$\mathbf{K}_{aa} = \mathbf{K}^0_{aa} - (\mathbf{K}^0_{ia})^{\mathrm{T}}(\mathbf{K}^0_{ii})^{-1}\mathbf{K}^0_{ia},\ \mathbf{K}_{ab} = \mathbf{K}^0_{ab} - (\mathbf{K}^0_{ia})^{\mathrm{T}}(\mathbf{K}^0_{ii})^{-1}\mathbf{K}^0_{ib},\ \mathbf{K}_{bb} = \mathbf{K}^0_{bb} - (\mathbf{K}^0_{ib})^{\mathrm{T}}(\mathbf{K}^0_{ii})^{-1}\mathbf{K}^0_{ib}$$

$$\mathbf{p}^*_a = \mathbf{p}_{ae} - (\mathbf{K}^0_{ia})^{\mathrm{T}}(\mathbf{K}^0_{ii})^{-1}\mathbf{p}_{ie} \quad \mathbf{p}^*_b = \mathbf{p}_{be} - (\mathbf{K}^0_{ib})^{\mathrm{T}}(\mathbf{K}^0_{ii})^{-1}\mathbf{p}_{ie}$$

Considering the displacements and forces as state vectors

$$\mathbf{y}_a = \begin{Bmatrix}\mathbf{u}_a\\ \mathbf{p}_a\end{Bmatrix}, \mathbf{y}_b = \begin{Bmatrix}\mathbf{u}_b\\ \mathbf{p}_b\end{Bmatrix} \tag{4}$$

when the substructure has no external loads (i.e. $\mathbf{p}_{ae} = \mathbf{p}_{be} = \mathbf{p}_{ie} = 0$), equation (3) takes the following form in state space

$$\mathbf{y}_b = \mathbf{S}(\omega)\mathbf{y}_a \tag{5}$$

where

$$\mathbf{S}_{aa} = -\mathbf{K}^{-1}_{ab}\mathbf{K}_{aa}, \mathbf{S}_{ab} = \mathbf{K}^{-1}_{ab}$$

$$\mathbf{S}_{ba} = -(\mathbf{K}_{ab})^{\mathrm{T}} + \mathbf{K}_{bb}\mathbf{K}^{-1}_{ab}\mathbf{K}_{aa}, \mathbf{S}_{bb} = -\mathbf{K}_{bb}\mathbf{K}^{-1}_{ab}$$

It has been proved[15] that $\mathbf{S}$ is a symplectic matrix, that is

$$\mathbf{S}^{-\mathrm{T}} = \mathbf{J}\mathbf{S}\mathbf{J}^{-1} \quad \text{or} \quad \mathbf{S}^{\mathrm{T}}\mathbf{J}\mathbf{S} = \mathbf{J} \tag{6}$$
$$\mathbf{J} = \begin{bmatrix} \mathbf{0} & \mathbf{I}_n \\ -\mathbf{I}_n & \mathbf{0} \end{bmatrix}$$

where $\mathbf{J}$ is a unit symplectic matrix and $\mathbf{I}_n$ is the n-order unit matrix. Thus, if $\mathbf{S}(\omega)$ has $2n$ eigenvalues, if μ is an eigenvalue of $\mathbf{S}(\omega)$, then so is $1/\mu$. These eigenvalues are called propagation coefficients because they express the wave propagation characteristics. Now let the $2n$ eigenvalues be separated into two groups

$$\begin{aligned} &\text{(a) } \mu_i \quad i = 1, 2, \ldots, n; \quad |\mu_i| \le 1 \\ &\text{(b) } \mu_{n+i} = 1/\mu_i \quad i = 1, 2, \ldots, n, \quad |\mu_{n+i}| \ge 1 \end{aligned} \tag{7}$$

The corresponding eigenvectors can then be used to constitute the matrix

$$\mathbf{\Phi} = [\,\boldsymbol{\varphi}_1, \quad \boldsymbol{\varphi}_2, \quad \ldots, \quad \boldsymbol{\varphi}_{2n}\,] \equiv \begin{bmatrix} \mathbf{X}_a & \mathbf{X}_b \\ \mathbf{N}_a & \mathbf{N}_b \end{bmatrix} \tag{8}$$

The state vector $\mathbf{y}$ at each interface can be expanded in terms of the eigenvectors as

$$\mathbf{y} = \sum_{i=1}^{n} (\alpha_i \boldsymbol{\varphi}_i + \beta_i \boldsymbol{\varphi}_{i+n}) \tag{9}$$

The coefficients α_i and β_i are rewritten in vector forms $\boldsymbol{\alpha}$ and $\boldsymbol{\beta}$. Numbering the substructures ..., -2, -1, 0, 1, 2,..., if an external harmonic load acts on substructure 0, it will generate two waves which propagate to its left and right, respectively. Once the coefficients $\boldsymbol{\alpha}$ and $\boldsymbol{\beta}$ for substructure 0 have been obtained, it is possible to obtain the response in any other substructure k, where positive k is to the right of the loaded substructure and negative k is to its left

$$\mathbf{y}_{kr} = \begin{bmatrix} \mathbf{X}_a \\ \mathbf{N}_a \end{bmatrix} \boldsymbol{\mu}^k \boldsymbol{\alpha} \quad k > 0$$
(the right of the loaded substructure) (10)

$$\mathbf{y}_{kl} = \begin{bmatrix} \mathbf{X}_b \\ \mathbf{N}_b \end{bmatrix} \boldsymbol{\mu}^{-k} \boldsymbol{\beta} \quad k < 0$$
(the left of the loaded substructure) (11)

where $\boldsymbol{\mu} = \mathrm{diag}[\mu_1, \mu_2, ..., \mu_n]$

For the substructure which is subjected to the harmonic excitation, that is, $k = 0$, equations (10) and (11) give

$$\mathbf{u}_a = \mathbf{X}_b\boldsymbol{\beta}, \mathbf{p}_a = \mathbf{N}_b\boldsymbol{\beta}, \mathbf{u}_b = \mathbf{X}_a\boldsymbol{\alpha}, \mathbf{p}_b = \mathbf{N}_a\boldsymbol{\alpha} \tag{12}$$

Substituting equation (12) into equation (3) yields the equation of motion denoted by the symplectic modal coordinate $[\boldsymbol{\beta}^{\mathrm{T}}, \boldsymbol{\alpha}^{\mathrm{T}}]^{\mathrm{T}}$ as

$$\begin{bmatrix} \mathbf{K}_{aa} - \mathbf{N}_b\mathbf{X}_b^{-1} & \mathbf{K}_{ab} \\ \mathbf{K}_{ab}^{\mathrm{T}} & \mathbf{K}_{bb} + \mathbf{N}_a\mathbf{X}_a^{-1} \end{bmatrix} \begin{bmatrix} \mathbf{X}_b & \mathbf{0} \\ \mathbf{0} & \mathbf{X}_a \end{bmatrix} \begin{Bmatrix} \boldsymbol{\beta} \\ \boldsymbol{\alpha} \end{Bmatrix} = \begin{Bmatrix} \mathbf{p}_a^* \\ \mathbf{p}_b^* \end{Bmatrix} \tag{13}$$

Therefore, a periodic chain substructure can be chosen to analyze the vertical vibration of an adjacent building instead of an infinitely long pavement model.

Vibration analysis and MEM

A substructure of length l has been established to derive the dynamic equations of the pavement–vehicle coupling system, where l is long enough to include the vehicle wheelbase and the distance from the vehicle to the adjacent building.

In this mechanical model, the vehicle is regarded as a spring–mass–damper system with 4 degrees of freedom, namely, the vertical motion of the vehicle body, rotation in the $x - z$ plane, and vertical motions of the front and rear wheels. The pavement supporting structure is regarded as three layers of discrete point supports, namely, the pavement plate, elastic damping layer, and foundation layer. The road surface unevenness $r(x)$ is a stationary random process varying with x. In order to conveniently analyze the dynamic characteristics of the system, a moving load method is used to derive its discrete equations. D'Alembert's principle gives the differential equations of motion of the model of Figure 1 as

$$D\nabla^2\nabla^2 u_u + \mu u_u + \eta\frac{\partial u_u}{\partial t} + m\frac{\partial^2 u_u}{\partial t^2} = p(t)\delta(x - Vt) \tag{14}$$

where ∇^2 is the Laplacian; $u_u = u_u(x, y, t)$ represents the displacements of the pavement plate and buildings; $D = Eh^3/12(1 - \upsilon)$ is the plate flexural rigidity; h, E, υ, and m are, respectively, the thickness, elastic modulus, Poisson's ratio, and mass per unit area of the plate; $p(t)$ is the external load; μ and η are the rigidity and damping of the foundation, respectively; and V denotes the speed of the moving load.

For single-point or multi-support excitation models, it is effective to change the moving vehicle load into contacting pavement elements by assuming a moving coordinate, as shown in Figure 4. Based on the 2D MEM,[16] the elements are formulated in a relative coordinate system attached to the moving vehicle. These are not physical elements attached to the material, but are conceptual elements that "flow" along the pavement with the moving vehicle. The main advantage is that the

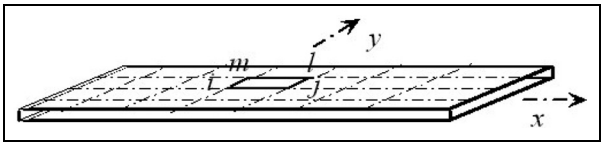

Figure 4. Discretization of plate into moving elements.

moving vehicle is relatively static in this coordinate system and does not cross from one element into another, thereby avoiding the updating of force and displacement vectors due to the change in contact point on the elements.

Now consider a typical moving rectangular element of length a and width b, with nodes i, j, m, and l. Define the moving coordinates X, Y as

$$X = x - Vt, \quad Y = y \tag{15}$$

Then the equation of motion of this moving element can be expressed as

$$D\nabla^2\nabla^2 u_u + \mu u_u + \eta\left(\frac{\partial u_u}{\partial t} - V\frac{\partial u_u}{\partial X}\right) + m\left(\frac{\partial^2 u_u}{\partial t^2} - 2V\frac{\partial^2 u_u}{\partial t \partial X} + V^2\frac{\partial^2 u_u}{\partial X^2}\right) = p\delta(X) \tag{16}$$

Using the FEM, the deflection u_u can be expressed by the nodal displacement vector $\mathbf{u}_u^e$ as

$$u = \mathbf{N}\mathbf{u}_u^e \tag{17}$$

where $\mathbf{N}$ is the shape function vector, which for a Kirchhoff plate element with Kelvin foundation can be written as

$$\mathbf{N} = \{N_i, N_{x_i}, N_{y_i}, N_j, N_{x_j}, N_{y_j}, N_m, N_{x_m}, N_{y_m}, N_l, N_{x_l}, N_{y_l}\} \tag{18}$$

$$N_k = (1+\xi_0)(1+\psi_0)(2+\xi_0+\psi_0-\xi^2-\psi^2)/8$$
$$N_{x_k} = -b\psi_k(1+\xi_0)(1+\psi_0)(1-\psi^2)/8$$
$$N_{y_k} = -a\xi_k(1+\xi_0)(1+\psi_0)(1-\xi^2)/8$$

in which

$$k = i,j,m,l; \quad \xi = (x-x_c)/a; \quad \psi = (y-y_c)/b; \quad \xi_0 = \xi\xi_k; \quad \psi_0 = \psi\psi_k$$

where x_c and y_c are the central coordinates of the element in moving coordinate. Note that most of the elements do not contact with any loads, and for such elements, the force terms on the right-hand side of the equations of motion vanish. Using Galerkin's approach, equation (16) is multiplied by a weighting function $\mathbf{N}$ and is integrated over the surface of the plate element. The weak Galerkin form can be obtained as

$$\iint_s \mathbf{N}\left[D\nabla^2\nabla^2 u_u + \mu u_u + \eta\left(\frac{\partial u_u}{\partial t} - V\frac{\partial u_u}{\partial X}\right)\right] + \iint_s \mathbf{N}\left[m\left(\frac{\partial^2 u_u}{\partial t^2} - 2V\frac{\partial^2 u_u}{\partial t\partial X} + V^2\frac{\partial^2 u_u}{\partial X^2}\right) - p\delta(X)\right] = 0 \tag{19}$$

Substituting equations (17) and (18) into equation (19) gives

$$\begin{aligned}&\iint_s (\mathbf{B}^T\mathbf{D}\mathbf{B})\mathbf{u}_u^e ds + \iint_s \mu\mathbf{N}^T\mathbf{N}\mathbf{u}_u^e ds \\ &+ \iint_s \eta\left(\frac{\partial \mathbf{u}_u^e}{\partial t}\mathbf{N}^T\mathbf{N} - V\frac{\partial \mathbf{N}^T}{\partial X}\mathbf{N}\mathbf{u}_u^e\right) ds \\ &+ \iint_s m\left(\frac{\partial^2 \mathbf{u}_u^e}{\partial t^2}\mathbf{N}^T\mathbf{N} - 2V\frac{\partial \mathbf{u}_u^e}{\partial t}\frac{\partial \mathbf{N}^T}{\partial X}\mathbf{N} + V^2\frac{\partial^2 \mathbf{N}^T}{\partial X^2}\mathbf{N}\mathbf{u}_u^e\right) ds \\ &- \iint_s \mathbf{N}p\delta(X) ds = 0\end{aligned} \tag{20}$$

$$\mathbf{B} = -\begin{bmatrix} \frac{\partial^2 N_i}{\partial x^2} & \frac{\partial^2 N_{x_i}}{\partial x^2} & \frac{\partial^2 N_{y_i}}{\partial x^2} & \cdots & \frac{\partial^2 N_{y_l}}{\partial x^2} \\ \frac{\partial^2 N_i}{\partial y^2} & \frac{\partial^2 N_{x_i}}{\partial y^2} & \frac{\partial^2 N_{y_i}}{\partial y^2} & \cdots & \frac{\partial^2 N_{y_l}}{\partial y^2} \\ 2\frac{\partial^2 N_i}{\partial x\partial y} & 2\frac{\partial^2 N_{x_i}}{\partial x\partial y} & 2\frac{\partial^2 N_{y_i}}{\partial x\partial y} & \cdots & 2\frac{\partial^2 N_{y_l}}{\partial x\partial y} \end{bmatrix}$$

$$\mathbf{D} = \frac{Eh^3}{12(1-\upsilon)}\begin{bmatrix} 1 & \upsilon & 0 \\ \upsilon & 1 & 0 \\ 0 & 0 & (1-\upsilon)/2 \end{bmatrix}$$

It can be shown that the element mass $\mathbf{M}_e$, damping $\mathbf{C}_e$, and stiffness $\mathbf{K}_e$ matrices in the moving coordinate system are, respectively[16]

$$\mathbf{K}_e = \iint_s \mathbf{B}\mathbf{D}\mathbf{B} ds + \mu\iint_s \mathbf{N}^T\mathbf{N} ds - V\eta\iint_s \frac{\partial \mathbf{N}^T}{\partial x}\mathbf{N} ds + mV^2\iint_s \frac{\partial^2 \mathbf{N}^T}{\partial x^2}\mathbf{N} ds \tag{21}$$

$$\mathbf{C}_e = \eta\iint_s \mathbf{N}^T\mathbf{N} ds - 2Vm\iint_s \frac{\partial \mathbf{N}^T}{\partial X}\mathbf{N} ds \tag{22}$$

$$\mathbf{M}_e = m\iint_s \mathbf{N}^T\mathbf{N} ds \tag{23}$$

Assembling all the element matrices gives the equations of motion of the pavement

$$\mathbf{M}\ddot{\mathbf{u}} + \mathbf{C}\dot{\mathbf{u}} + \mathbf{K}\mathbf{u} = \mathbf{F}(t) = \mathbf{F}_1 + \mathbf{F}_2 \tag{24}$$

Here, $\mathbf{F}$ is the excitation vector which includes two terms, $\mathbf{F_1}$ caused by the vehicle weight and $\mathbf{F_2}$ related to the random road roughness. The response induced by $\mathbf{F_1}$ is deterministic and is easily obtained by numerical methods. In this article, we focus on the random vibration characteristic of the coupling system caused by $\mathbf{F_2}$. It can be reasonably assumed that the excitations aroused by the pavement surface irregularity are

stationary Gaussian processes with the power spectrum density (PSD) matrix denoted as $\mathbf{S}_r(\Omega)$ in space-domain. According to random vibration theory, the PSD matrix $\mathbf{S}_r(\Omega)$ can be denoted as $\mathbf{S}_r(\omega)$ in time-domain in equation (25); $\mathbf{S}_r(\omega)$ be expressed as equation (26) based on GB7031[17]

$$\mathbf{S}_r(\omega) = \frac{1}{V}\mathbf{S}_r(\Omega) \tag{25}$$

$$\mathbf{S}_r(\omega) = \frac{2\pi S_q(n) n_0^2 V}{\omega^2} \tag{26}$$

where n is a spatial frequency (m^{-1}); n_0 is its reference value, with $n_0 = 0.1\,\mathrm{m}^{-1}$ usually used; $S_q(n_0)$ is the PSD value at frequency n_0 and is related to the road grade. $\mathbf{u} = \{u_1 \quad u_2 \quad \ldots \quad u_n\}$ is the nodal displacement vector. Using MEM, the load speed, foundation damping, and rigidity are all coupled with the element matrices, and, as will be seen below, equation (24) can easily be computed because it is linear and time-independent.

PEM of moving element

For the coupled random vibration of equation (24), the response power spectral density (PSD) matrix can be expressed as[18]

$$\mathbf{S}_{out}(\omega) = \mathbf{H}^*(\omega)\mathbf{S}_{in}(\omega)\mathbf{H}^{\mathrm{T}}(\omega) \tag{27}$$

where $\mathbf{S}_{in}(\omega)$ and $\mathbf{S}_{out}(\omega)$ are the PSD matrices of the excitation and response vectors, respectively; $\mathbf{H}(\omega)$ is the frequency response matrix and the superscript * denotes the conjugate of a matrix, and ω is time-domain frequency. In fact, at the pavement–wheel contact points, the excitations can be regarded as fully coherent, and so can be transformed into a sinusoidal excitation based on the PEM, thus considerably simplifying the computation without losing any accuracy.

In the vehicle–pavement computational model, $\mathbf{F_2}$ can be expressed as

$$\mathbf{r}(x) = \{r(x), r(x - l_t)\}^{\mathrm{T}} \tag{28}$$

where l_t is the distance between the two wheels, and $\mathbf{r}(x)$ is the pavement surface irregularity, composed of the front wheel location excitation $r(x)$ and the rear wheel $r(x - l_t)$. Assuming $S_r(\Omega)$ is the PSD of $\mathbf{r}(x)$, then

$$S_r(\omega) = \frac{S_r(\Omega)}{V}; \quad \omega = \Omega V \tag{29}$$

where $S_r(\omega)$ and $S_r(\Omega)$ are the PSD of the pavement surface irregularity excitation, ω is the time-domain frequency and Ω is the space-domain frequency. The pseudo-harmonic excitation is constituted as

$$\tilde{\mathbf{r}}(t) = \{\tilde{r}_1, \tilde{r}_2\}^{\mathrm{T}} = \{e^{-i\omega t_1}, e^{-i\omega t_2}\}^{\mathrm{T}}\sqrt{S_r(\omega)}e^{i\omega t} \tag{30}$$

$$t_1 = 0,\ t_2 = \frac{l_t}{V}$$

where $\tilde{r}_1$ and $\tilde{r}_2$ denote the pseudo-sinusoidal excitation of the pavement in the front and the rear wheel location, respectively, and t_1 and t_2 are the time difference. The input PSD $\mathbf{S}_{in}(\omega)$ and output PSD $\mathbf{S}_{out}(\omega)$ can be expressed as

$$\mathbf{S}_{in}(\omega) = \tilde{\mathbf{r}}^*\tilde{\mathbf{r}}^{\mathrm{T}}, \mathbf{S}_{out}(\omega) = \tilde{\mathbf{u}}^*\tilde{\mathbf{u}}^{\mathrm{T}} \tag{31}$$

Note that it is assumed that $S_r(\Omega)$ is known, and equation (30) means that the coupled system has many deterministic harmonic excitation components corresponding to different Ω as its inputs. Clearly, when PEM is used, it is very efficient because the computation only involves the solution of linear equations and vector multiplications.

Numerical example

Computational model and parameters

A simplified model of a coupled vehicle–bridge system is shown in Figure 1. Assume the vehicle moves in the x-direction (at $y = 0$) on the smooth pavement with velocity V. The pavement substructure length is $l = 60\,\mathrm{m}$. The adjacent building is a three-story slab structure for which Rayleigh damping is used. The parameters for the vehicle,[19] pavement, and adjacent building are listed in Table 1. The PSD for the roughness of the pavement surface is given by the Chinese national standard (GB7031), which can be expressed as equation (26), where V is the vehicle velocity, n_0 is a reference frequency (usually $n_0 = 0.1\,\mathrm{m}^{-1}$ is assumed), and G_q is a coefficient related to the road grade ($G_q = 6.4 \times 10^{-6}\,\mathrm{m}^2\,\mathrm{m}^{-1}$ for Grade B; $G_q = 25.6 \times 10^{-6}\,\mathrm{m}^2\,\mathrm{m}^{-1}$ for Grade C).

Computational results and response analysis

Using a self-compiling program in MATLAB 6.5,[20] the vibration responses of the three subsystems are obtained and shown in Figures 5–9. Figure 5 shows the three-dimensional deflected shape of the pavement. It can be seen that the deflected shape is a strip deformation and it is influenced considerably by the moving speed. The responses of the pavement and the belt of folded strata adjacent to the building are relatively strong, because the building's larger rigidity enhances the pavement stiffness. Correspondingly, the response amplitude on the other side is much weaker.

Figure 6 shows the PSD of vehicle body vertical acceleration when the road condition is Grade B. It shows two peaks, the first peak just below 2 Hz and the second at about 6 Hz, which are caused by the phase difference of wheel excitations.

Table 1. Vehicle, pavement, and building parameters.

Parameter	Value
Vehicle model[18]	
Mass of the vehicle body	$m_c = 708\,\text{kg}$
Masses of vehicle front or rear wheel	$m_r = m_f = 80\,\text{kg}$
Rotational inertias	$J = 1060\,\text{kg m}^2$
Rear stiffness coefficient	$k_r = 19,326\,\text{N/m}$
Front stiffness coefficient	$k_f = 20,292\,\text{N/m}$
Rear and front damping coefficients	$c_r = c_f = 1000\,\text{N s/m}$
Distance from rear wheel to core	$lr = 1.308\,\text{m}$
Distance from front wheel to core	$l_f = 1.168\,\text{m}$
Tire stiffness coefficient	$wk_r = wk_f = 128,760\,\text{N/m}$
Pavement model	
Elastic modulus	$E = 1.516\times10^{10}\,\text{Pa}$
Poisson's ratio	$\upsilon = 0.35$
Mass per unit area	$\rho = 3.66\times10^2\,\text{kg/m}^2$
Plate thickness	$h = 0.15\,\text{m}$
Foundation reaction modulus	$\mu = 9.5\times10^7\,\text{N/m}^3$
Foundation damping coefficient	$\eta = 1400\,\text{kN s/m}^2$
Building model	
Floors	3
Story height	$h_l = 3\,\text{m}$
Floor thickness	$t_l = 0.15\,\text{m}$
Column cross-sectional area	$A_p = 0.8\,\text{m}^2$
Elastic modulus	$E_c = 2.5\times10^{10}\,\text{N/m}$
Mass per unit length	$\rho_l = 2.5\times10^3\,\text{kg/m}$
Vertical rigidity at contact points	$k_{ve} = 1.0\times10^9\,\text{N/m}$
Damping at contact points	$c_{ve} = 3.475\times10^6\,\text{N s/m}$

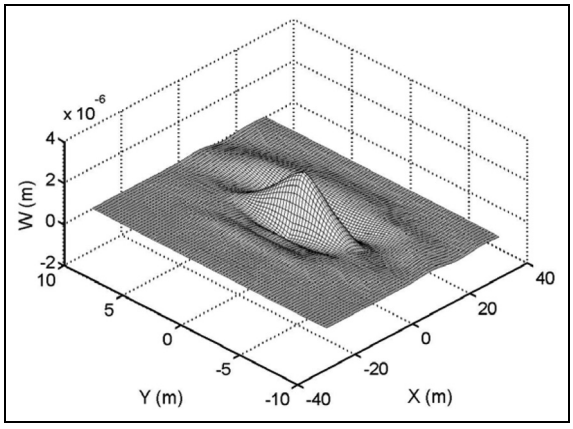

Figure 5. Three-dimensional deflected shape of the pavement.

Figures 7–9 give the vertical vibration responses of the adjacent building, which are induced by the vehicle–pavement coupling system, respectively, including the building mid-acceleration responses, vertical acceleration PSD, and mean vertical displacement. The mid-acceleration means of different floors can be compared in Figure 7, where it is seen that the resonance frequency is the same for the first and third floors, and that the amplitude of the first floor is bigger. It is also found that the responses of the building become

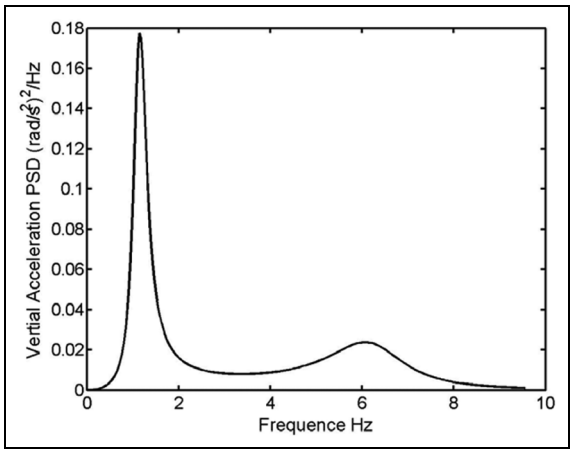

Figure 6. Vehicle vertical acceleration PSD.

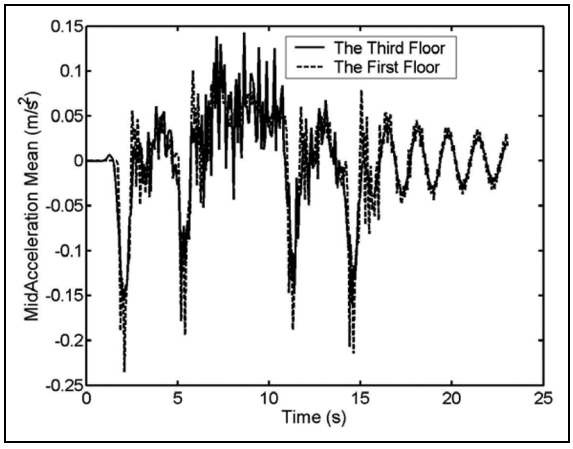

Figure 7. Building mid-acceleration responses.

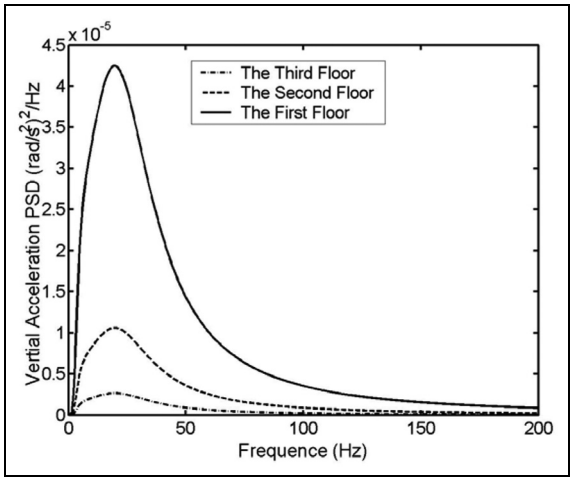

Figure 8. Building vertical acceleration PSD.

stronger as the vehicle approaches it and decrease as the vehicle leaves, and the response differences between different floors gradually vanish. Because of the damping

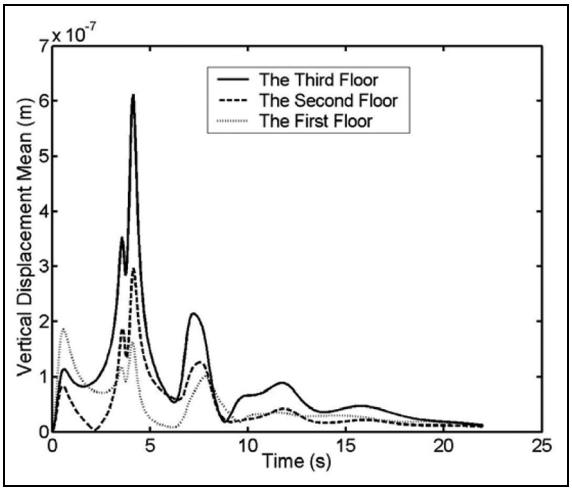

Figure 9. Building mean vertical displacement.

effect of the building structure, the vibration is gradually damped out.

Figure 8 gives the vertical acceleration PSD of different floors. The results show that the response peaks of the building are located near 20 Hz. This characteristic remains unchanged while the vibration accelerations decrease with increasing floor height, which reflects the energy attenuation of the wave. Figure 9 gives the mean vertical displacements of different floors and shows that the peaks of mean displacement increase as the mid-acceleration responses increase. In contrast, the variations in the response peaks increase with increasing height.

Conclusion

This article establishes an integrated numerical model for traffic-induced environmental vibration, including vibration source, propagation path, and a vibrated building. A periodic chain substructure is used to simplify the infinitely long pavement. The 2D MEM is derived to change the non-stationary random vibration into quasi-static dynamic functions in each substructure. PEM and symplectic methodology have been combined to study the dynamic behavior of the complex system. The numerical example has verified the feasibility and efficiency of the proposed method. The following conclusions can be drawn:

1. The periodic chain substructure for a damped vehicle–pavement system is proved to be suitable for analyzing the random responses of an adjacent building. The model truncation errors induced by artificial boundaries are avoided and, because the calculation scale is decreased, computational accuracy is enhanced.
2. For complex non-stationary multiple point excitation, by means of the MEM, the vehicle speed, foundation damping, and rigidity all are coupled into the element matrix, and because the system remains linear and time-independent, the computational efficiency is significantly improved.
3. The characteristics of building responses induced by traffic load obviously change with the distance of the vehicle from the building. The responses of different floors are affected considerably by the hysteretic damping of the building, particularly in the high-frequency region. As the pavement stiffness is strengthened around the building, the responses on this side are stronger than those on the other side.

In addition, this article focuses on developing an efficient computational method and a reasonable model for analysis, and so some assumptions have been made. Further research will be done to verify such assumptions, and the experimental data will be developed.

Declaration of conflicting interests

The author(s) declared no potential conflicts of interest with respect to the research, authorship, and/or publication of this article.

Funding

The author(s) disclosed receipt of the following financial support for the research, authorship, and/or publication of this article: The authors are grateful for financial support from the National Natural Science Foundation (NSF) of China (grant no 11402235) and the Cardiff Advanced Chinese Engineering Centre.

References

1. Jones CJC and Block JR. Prediction of ground vibration from freight trains. *J Sound Vib* 1996; 193: 205–213.
2. Degrande G and Lombaert G. High-speed train induced free vibrations: in situ measurements and numerical modeling. In: *Proceedings of the Wave 2000*, Bochum, 13–15 December 2000, pp.29–42.
3. Hayakawa K, Kani Y, Matsubara N, et al. Ground vibrations isolation by PC wall piles. In: *Proceedings of the 4th International Conference on Case Histories in Geotechnical Engineering (ICCHGE)*, St. Louis, Missouri, 1998, pp.662–667.
4. Xu QY, Qu X, Au FTK, et al. Effects of track irregularities on environmental vibration caused by underground railway. *Eur J Mech A: Solid* 2016; 59: 280–293.
5. Alves CP, Calcada R and Silva CA. Track–ground vibrations induced by railway traffic: in-situ measurements and validation of a 2.5D FEM-BEM model. *Soil Dyn Earthq Eng* 2012; 32: 111–128.
6. Cao YM, Xia H, Lu WL, et al. A numerical method to predict the riding comfort induced by foundation

construction close to a high-speed-line bridge. *Proc IMechE, Part F: J Rail and Rapid Transit* 2015; 229: 553–564.
7. Wang KP, Xia H, Xu M, et al. Dynamic analysis of train-bridge interaction system with flexible car-body. *J Mech Sci Technol* 2015; 29: 3571–3580.
8. Chen G and Zhai WM. A new wheel/rail spatially dynamic coupling model and its verification. *Vehicle Syst Dyn* 2004; 41: 301–322.
9. Zhai WM, He ZX and Song XL. Prediction of high-speed train induced ground vibration based on train-track-ground system model. *Earth Eng & Eng Vib* 2010; 9: 545–554.
10. Yang YB and Hung HH. A 2.5D finite/infinite element approach for modelling visco-elastic bodies subjected to moving loads. *Int J Numer Meth Eng* 2003; 51: 1317–1336.
11. Connolly DP, Kouroussis G, Laghrouche O, et al. Benchmarking railway vibrations—track, vehicle, ground and building effects. *Constr Build Mater* 2015; 92: 64–81.
12. Tao XX and Wang GX. Rupture directivity and hanging wall effect in near field strong ground motion simulation. *Acta Seismol Sin* 2003; 16: 205–212.
13. Xu WT, Lin JH, Zhang YH, et al. 2D moving element method for random vibration analysis of vehicles on Kirchhoff plate with Kelvin foundation. *Lat Am J Solids Stru* 2009; 6: 169–183.
14. Lu F, Kennedy D, Williams FW, et al. Symplectic analysis of vertical random vibration for coupled vehicle–track systems. *J Sound Vib* 2008; 317: 236–249.
15. Zhong WX and Williams FW. The eigensolutions of wave propagation for repetitive structures. *Struct Eng Mech* 1993; 1: 47–60.
16. Koh CG, Ong JSY, Chua DKH, et al. Moving element method for train-track dynamics. *Int J Numer Meth Fl* 2003; 56: 1549–1567.
17. Yu ZS. *Vehicle theory*. Beijing, China: China Machine Press, 2000.
18. Lin JH, Zhang YH, Li XS, et al. Seismic spatial effects for long-span bridges, using the pseudo excitation method. *Eng Struct* 2004; 26: 1207–1216.
19. Zhang LL, Tang JS and Li LB. Transient dynamic response analysis of a thin-walled conical shell. *J Vib Shock* 2006; 25: 168–187 (in Chinese).
20. *MATLAB*. Natick: The MathWorks Inc., 2012.